

© 2024 IEEE. Personal use of this material is permitted. Permission from IEEE must be obtained for all other uses, including reprinting/republishing this material for advertising or promotional purposes, collecting new collected works for resale or redistribution to servers or lists, or reuse of any copyrighted component of this work in other works. This work has been submitted to the IEEE for possible publication. Copyright may be transferred without notice, after which this version may no longer be accessible.

System-Level Performance Metrics Sensitivity of an Electrified Heavy-Duty Mobile Manipulator

Mohammad Bahari*, Alvaro Paz, and Jouni Mattila

Faculty of Engineering and Natural Sciences, Tampere University, 33720, Finland

*Email: mohammad.bahari@tuni.fi

Abstract—The shift to electric and hybrid powertrains in vehicular systems has propelled advancements in mobile robotics and autonomous vehicles. This paper examines the sensitivity of key performance metrics in a electrified heavy-duty mobile manipulator (HDMM) driven by electromechanical linear actuators (EMLAs) powered by permanent magnet synchronous motors (PMSMs). The study evaluates power delivery, force dynamics, energy consumption, and overall efficiency of the actuation mechanisms. By computing partial derivatives (PD) with respect to the payload mass at the tool center point (TCP), it provides insights into these factors under various loading conditions. This research aids in the appropriate choice or design of EMLAs for HDMM electrification, addressing actuation mechanism selection challenge in vehicular system with mounted manipulator and determines the necessary battery capacity requirements.

Index Terms—electric powertrains, electromechanical linear actuator (EMLA), energy efficiency in vehicular systems, heavy-duty mobile manipulators (HDMMs), performance metrics, robotic vehicular actuation mechanism.

NOMENCLATURE

List of Abbreviations

DoF	Degree-of-freedom
EHLA	Electrohydraulic linear actuator
EMLA	Electromechanical linear actuator
EM	Electric motor
EV	Electric vehicle
HDMM	Heavy-duty mobile manipulator
ICE	Internal combustion engine
OHM	Off-highway machines
PD	Partial derivative
PMSM	Permanent magnet synchronous motor
RNEA	Recursive Newton-Euler algorithm
TCP	Tool center point

List of Symbols

Ψ	Sensitivity metrics
η	Efficiency of the mechanism
ω	Angular velocity (rad/s)
ψ_{PM}	Magnetic flux of permanent magnet (Wb)
ρ	Screw lead (m)
τ	Torque (N · m)
b	Viscous friction (N · s/m) or (N · m · s/rad)
e	Back EMF of electric motor (V)
F	Force (N)
i	Stator current of electric motor (A)

j	Inertia (kg · m ²)
k	Stiffness (N/m) or (N · m/rad)
L	Stator inductance of electric motor (H)
m	Mass (kg)
N	Ratio
n_p	Number of pole pairs
n_{ph}	Number of electric motor phases
p	Number of pole pairs
R	Stator resistance of electric motor (Ω)
V	Voltage of the electric motor (V)
v	Linear velocity (m/s)
V_{dc}	DC voltage of the inverter (V)
S_n	Switch commands (n=1, 2, ..., 2 n_{ph})

List of Subscripts

d, q	Related to the d- and q-axis
eq	Equivalent value
g	Indicating the parameters related to gearbox
l	Indicating the parameters related to load side
m	Indicating the parameters related to electric motor
p	Indicating the parameters related to planetary gear
s	Indicating the parameters related to screw mechanism
UVW	Indicating the phase of electric motor

I. INTRODUCTION

A. Background and Motivations

The growing urgency to address climate change and environmental degradation, driven by greenhouse gases like CO₂, has led to a global shift towards sustainability. International agreements such as the Paris Agreement 2015 and the EU's planned ban on ICE vehicle sales by 2035 underscore the need for emission reduction and greener alternatives [1]. Transitioning to electric power, especially from renewable sources, offers an effective path to not only mitigating environmental impacts but also enhances operational efficiency. In the off-highway machines (OHMs) and heavy machinery sector, traditionally reliant on ICEs, electrifying powertrains represents a major technological advancement [2]. With a growing focus on sustainability, the shift towards electric vehicles (EVs), including OHMs, is accelerating due to several key benefits:

- **Substantial Emission Reductions:** Replacing ICEs with electric alternatives lowers emissions, aiding in global CO₂ reduction and compliance with environmental regulations, especially in heavy-duty applications.
- **Superior Energy Efficiency:** Electric powertrains are more energy-efficient than traditional ICEs, leading to reduced

This work was supported by Business Finland partnership project "Future all-electric rough terrain autonomous mobile manipulators" (Grant 2334/31/2022).

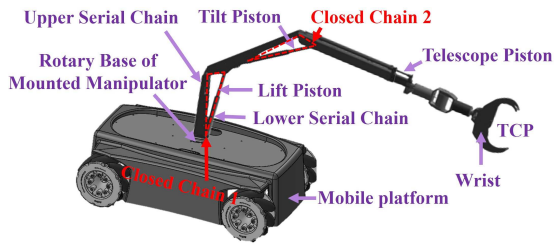


Fig. 1: Illustrative configuration of an electrified HDMM

TABLE I: Comparing different factors of EHLA and EMLA actuation technology

Characteristic	EHLA	EMLA
Energy efficiency	Moderate	High
Environmental impact	High	Low
Load capacity	High	Moderate
Temperature resilience	Low	High
Controllability	Moderate	High
Maintenance requirements	High	Low
Initial cost	Moderate	High
Overload tolerance	High	Moderate
Operation sound noise	Moderate	Quite

energy use and costs, crucial for HDMMs in energy-intensive fields like construction and mining.

- *Seamless Integration with Automation Technologies:* Electric powertrains' precision and control enable integration with advanced automation systems, fostering the development of intelligent HDMMs that enhance safety and productivity by automating complex tasks.
- *Reduced Maintenance/Operational Downtime:* With fewer moving parts than ICEs, electric powertrains require less maintenance and have lower operational downtime, beneficial for HDMMs working remotely.

Electrification is becoming crucial for the heavy machinery industry, especially for mobile working machines, which are key in sectors like manufacturing, logistics, agriculture, and search and rescue operations [3]. Integrating electric actuators aligns with sustainability goals and advances intelligent industrial systems. Fig. 1 shows a conceptual setup of an electrified HDMM with a mobile platform and mounted robotic manipulator, demonstrating the shift towards sustainable and autonomous heavy-duty operations. Two main options for electric actuators are electromechanical linear actuators (EMLAs) and electrohydraulic linear actuators (EHLAs). EHLAs offer high force and power-to-weight ratios but face challenges like control limitations, inefficiency from fluid incompressibility, and leakage [4]. In contrast, EMLAs provide greater precision and efficiency with programmable features that enhance control and reduce maintenance. They avoid energy conversion losses inherent in hydraulic systems, making them a greener choice [5]. For a detailed comparison, see Table I [6]. With the benefits of electrification and advancements in power electronics, driver technology, and electric motors, EMLAs powered by permanent magnet synchronous motors (PMSMs) are expected to significantly impact green vehicular systems,

especially for HDMMs since the adoption of PMSM lead to high torque density, high efficiency, better controllability, and low cogging torque [7], [8], making them ideal for HDMM applications. Ongoing research aims to optimize these systems to meet the rigorous demands of modern industrial practices.

B. Contributions and Structure of the Paper

This paper presents a comprehensive system-level sensitivity analysis of a heavy-duty mobile manipulator (HDMM) powered by electromechanical linear actuators (EMLAs) driven by permanent magnet synchronous motors (PMSMs). We develop a detailed model of the EMLA mechanism and generate a trajectory task for the robotic manipulator to ensure accurate tracking of the tool center point (TCP). The analysis evaluates various critical factors, including power delivery, force dynamics in the joint pistons, energy expenditure, and overall efficiency of the EMLAs. Additionally, we compute partial derivatives (PD) with respect to the payload mass at the TCP to examine how these factors vary under different loading conditions throughout the duty cycle. This study offers valuable insights into the performance and behavior of the EMLAs under diverse operational scenarios, aiding in the intelligent design and selection of EMLAs for each joint of the manipulator. Furthermore, it provides guidance for determining the necessary battery capacity to support the electrification of HDMMs. The organization of the paper is:

- The research begins with Section II, where we develop a detailed model of a gear-equipped PMSM-powered EMLA to analyze energy conversion processes. This model includes equivalent circuits for the inverter, EM, gearbox, screw mechanism, and load. Using the force-to-voltage and speed-to-current analogies, we provide a framework for understanding the governing dynamic of EMLA and analyzing its performance.
- In Section III-A, the method for generating motion for the studied EMLA-driven HDMM is described in detail, as presented in **Algorithm 1**. This second-order inverse differential kinematics algorithm outlines the process for generating motion. The algorithm updates the payload value in the *robot*(\cdot) data structure, performs time loop calculations for differential kinematics, computes the robot's inverse dynamics, and evaluates the sensitivity metrics (Ψ) based on linear velocities (v_{x_i}) and forces of the actuators (f_{x_i}) at the EMLA's load side.
- Section III-B presents the simulation and results of the sensitivity analysis on the 3-DoF EMLA-actuated HDMM, providing comprehensive insights into the behavior of the system with respect to the payload and pave the way for appropriate actuator sizing and determining required battery capacity for the HDMM.

II. MODELING AND ANALYSIS OF EMLA MECHANISM

In this paper, we develop the model of a gear-equipped PMSM-powered EMLA mechanism (see Fig. 2) to analyze governing dynamics. The model includes equivalent circuits of the inverter, motor, gearbox, screw mechanism, and load. We

use force-to-voltage and speed-to-current analogies to explore EMLA dynamics. By applying Park's transformation to the voltage equations and converting them to the dq reference frame, the equivalent circuits of the inverter-driven PMSM are obtained as shown in Fig. 3 and Fig. 4. The voltages (V_d and V_q) and the electromagnetic torque are expressed in (1) [9]:

$$\begin{cases} V_d = R_s i_d + L_d \frac{di_d}{dt} - p\omega_m L_q i_q \\ V_q = R_s i_q + L_q \frac{di_q}{dt} + p\omega_m i_d L_d + p\omega_m \Psi_{PM} \\ \tau_m = \frac{3}{2} n_p [i_q (i_d L_d + \Psi_{PM}) - i_d i_q L_q] \end{cases} \quad (1)$$

By obtaining the equivalent circuit of the EMLA, as depicted in Fig. 5, the dynamics of the mechanism can be captured. The general expression for the motor torque and EMLA dynamics are provided in (2) to integrate the mechanical part of the PMSM into the rest of EMLA components:

$$\begin{cases} \tau_m = a_{eq} \ddot{x}_L + b_{eq} \dot{x}_L + c_{eq} x_L + F_l \\ a_{eq} = \alpha^2 \left(\frac{m_s}{\alpha^2} + j_g + N_g^2 j_p + (N_g N_p)^2 j_m \right) \\ b_{eq} = b_s + (\alpha N_g N_p)^2 b_m \\ c_{eq} = \alpha^2 \left(\frac{1}{(N_p N_g)^2 k_{mp}} + \frac{1}{(N_g)^2 k_{pg}} + \frac{1}{k_{gs}} + \frac{1}{k_l} \right)^{-1} \\ \alpha = \frac{2\pi}{\rho} \end{cases} \quad (2)$$

Also, efficiency maps of EMLAs in the manipulator joints can be developed (see Fig. 6) by calculating power losses [10].

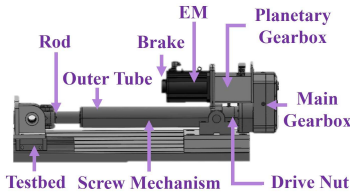


Fig. 2: EMLA structure and components

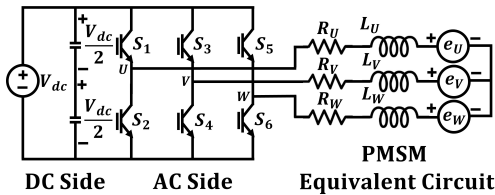


Fig. 3: Equivalent circuit of 3-phase PMSM

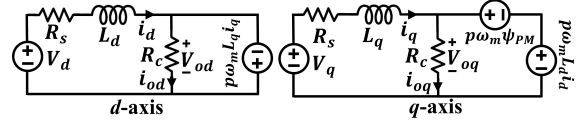


Fig. 4: Equivalent circuit of PMSM in dq-axis

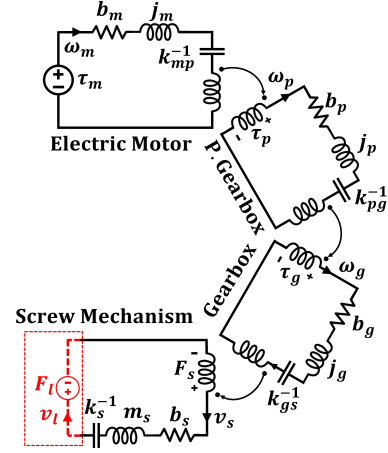


Fig. 5: Equivalent circuit of mechanical components of EMLA

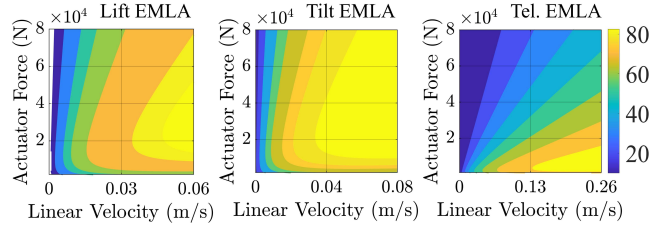


Fig. 6: Efficiency maps of EMLAs implemented in the lift, tilt, and telescope joints of the studied HDMM

III. SENSITIVITY OF PERFORMANCE METRICS IN HDMM

A. Manipulator Motion Generation

Our study focuses on heavy-duty parallel serial HDMM powered by EMLAs, as depicted in Fig. 1, capable of high-power tasks where payload analysis is crucial for actuator selection. The robot's configurational state is defined in its actuators' space as $\mathbf{q} \in \mathcal{R}^n$ where n is the number of DoF and number of mechanisms in the manipulator. Motion generation is performed via second-order inverse differential kinematics, as coded in **Algorithm 1**, where $\mathbf{x}_r(t)$, $\dot{\mathbf{x}}_r(t)$, and $\ddot{\mathbf{x}}_r(t)$ represent the position, velocity, and acceleration of a reference trajectory. The payload, assumed as a mass point in the robot's TCP reference frame, is denoted by m_{TCP} . To outline the algorithm, line 4 updates the payload in $robot(\cdot)$, containing all kinematic, inertial, and topological robot data. Line 5 initiates a time loop with final value M , where lines 7-9 compute the first and second-order differential inverse kinematics based on the reference trajectory. The manipulator Jacobian (\mathbf{J}) [11] and its first time derivative ($\dot{\mathbf{J}}$) are computed in lines 14-25. By following a screw theory notation [11],

[12]: s_i is the screw vector of the i -th actuator expressed at local coordinates, $\text{Ad}_{G_0^i}$ is the adjoint operator parameterized by the homogeneous transformation matrix $G_0^i \in SE(3)$ that represents the motion of frame i with respect to 0 frame, J^s is the spatial Jacobian, \dot{J}^s is its time derivative and the subscript $[:, i]$ refers to their i -th column. Also r_0^{TCP} is the distance vector from 0 reference frame to TCP frame and ad_{s_i} stands for the adjoint operator that performs a Lie bracket, see [13] for a detailed form of these adjoints operators. The superscript $+$ stands for the generalized pseudoinverse. Line 10 computes the robot's inverse dynamics [14] based on q , its first two time derivatives \dot{q} and \ddot{q} , and the $\text{robot}(\cdot)$ structure [15] [16]. The sensitivity metrics for this work are represented by Ψ which is computed in line 11 and it is a function of the linear velocities and forces of the actuators denoted by v_x and f_x , respectively.

B. Simulation and Results

The sensitivity analysis is conducted on a 3-DoF HDMM to monitor the behaviour of the performance metrics with respect to the payload. The parallel-serial manipulator under study is illustrated in Fig. 1, which is composed by two closed-kinematic chains and one telescope mechanism. The manipulator is forced to track a spiral reference trajectory that covers most of its operational space in a time of $M = 8\pi$ (s). We vary the payload m_{TCP} from 0 to 200 (kg) and perform the PD of Ψ with respect to m_{TCP} by means of finite differences with a payload perturbation factor of $\Delta_m = 2 \times 10^{-24}$ (kg), as (3).

$$\frac{\partial \Psi}{\partial m_{TCP}} \approx \frac{\Psi(m_{TCP} + \Delta_m) - \Psi(m_{TCP})}{\Delta_m} \quad (3)$$

The four scalar sensitivity metrics under study are defined as follows, computed and stacked in the variable Ψ for each EMLA at lift, tilt, and telescope, as itemized below:

- *Delivered power*: It is the power retrieved from the EMLA at an instant of time at the load side of actuator:

$$\psi_{1i} = v_{x_i} f_{x_i} \quad (4)$$

where v_{x_i} and f_{x_i} are the scalar linear velocity and force of the i -th actuator. The evaluation of the power metric (ψ_1) and its PD ($\partial \psi_1 / \partial m_{TCP}$) are depicted in Fig. 7.

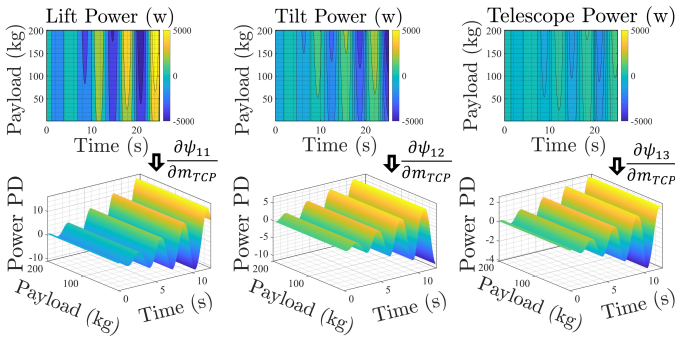


Fig. 7: Delivered power and its PD with respect to TCP payload in 3-DoF HDMM joints over time

- *Actuators' linear force*: The linear force exerted by the EMLA in the direction of motion at the load side:

$$\psi_{2i} = f_{x_i} \quad (5)$$

The assessment of the force metric (ψ_2) and its PD ($\partial \psi_2 / \partial m_{TCP}$) are shown in Fig. 8.

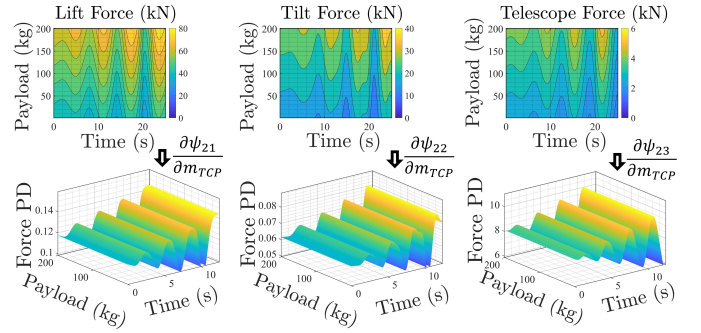


Fig. 8: Linear Force and its PD with respect to TCP payload in 3-DoF HDMM joints over time

- *Energy expenditure*: The total energy consumed by the EMLA over a period, calculated as the sum of the output power divided by the efficiency, integrated over time:

$$\psi_{3i} = \Delta_t \sum_{t=0}^M \frac{v_{x_i} f_{x_i}}{\eta_{\text{EMLA}_i}(f_{x_i}, v_{x_i})} \quad (6)$$

where Δ_t is the increment of time. Fig. 9 illustrates the energy metric (ψ_3) and its PD with respect to the TCP payload ($\partial \psi_3 / \partial m_{TCP}$).

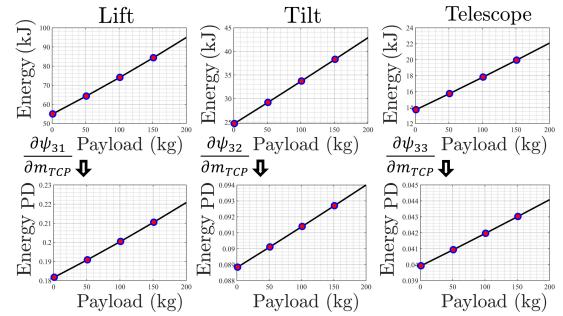


Fig. 9: Energy consumption and its PD with respect to TCP payload in 3 HDMM joints

- *Efficiency*: The efficiency of the EMLAs, calculated as the ratio of the output mechanical power to the input electrical power at an instant of time:

$$\psi_{4i} = \frac{v_{x_i} f_{x_i}}{\sqrt{3} V_{LL} I_{LL} \cos(\phi)} \quad (7)$$

Fig. 10 presents the efficiency metric (ψ_4) and its PD with respect to the TCP payload ($\partial \psi_4 / \partial m_{TCP}$).

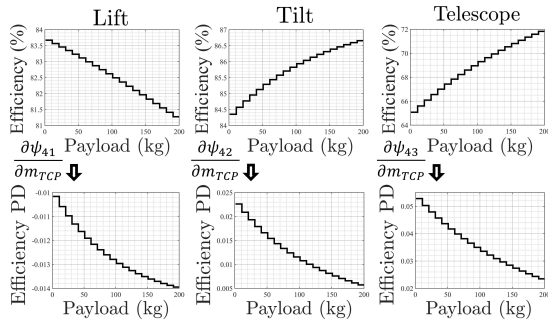


Fig. 10: Efficiency of EMLAs and its PD with respect to TCP payload in 3 HDMM joints

Algorithm 1: Second-Order Inverse Differential Kinematics

Input: $\mathbf{x}_r(t)$, $\dot{\mathbf{x}}_r(t)$, $\ddot{\mathbf{x}}_r(t)$, m_{TCP} .
Output: Ψ .

```

1  $\Psi \leftarrow \text{getMetrics}(\mathbf{x}_r(t), \dot{\mathbf{x}}_r(t), \ddot{\mathbf{x}}_r(t), m_{TCP})$ 
2  $\text{getMetrics}(\mathbf{x}_r(t), \dot{\mathbf{x}}_r(t), \ddot{\mathbf{x}}_r(t), m_{TCP})$ 
3 Initialize  $\mathbf{q}$ 
4 Update payload  $robot(m_{TCP})$ 
5 For  $t = 0 : M$  then
6    $[\mathbf{J}(t), \dot{\mathbf{J}}(t)] \leftarrow \text{getJacobian}(\mathbf{q}(t), \dot{\mathbf{q}}(t))$ 
7    $\dot{\mathbf{q}}(t) = \mathbf{J}^+(\mathbf{q}(t))\dot{\mathbf{x}}_r(t)$ 
8   Update  $\mathbf{q}(t)$ 
9    $\ddot{\mathbf{q}}(t) = \mathbf{J}^+(\mathbf{q}(t))[\ddot{\mathbf{x}}_r(t) - \dot{\mathbf{J}}(\mathbf{q}(t), \dot{\mathbf{q}}(t))\dot{\mathbf{q}}(t)]$ 
10   $[\mathbf{v}_x(t), \mathbf{f}_x(t)] \leftarrow \text{RNEA}(\mathbf{q}(t), \dot{\mathbf{q}}(t), \ddot{\mathbf{q}}(t), robot(m_{TCP}))$ 
11   $\Psi \leftarrow \text{evaluateMetrics}(\mathbf{v}_x(t), \mathbf{f}_x(t))$ 
12 end
13 end
14  $\text{getJacobian}(\mathbf{q}(t), \dot{\mathbf{q}}(t))$ 
15  $\text{Ad}_{G_0^0} \leftarrow \mathbf{0}$ 
16 For  $i = 1 : n$  then
17    $\mathbf{J}_{[:,i]}^s = \text{Ad}_{G_0^i} \mathbf{s}_i$ 
18    $\text{Ad}_{G_0^i} = \text{Ad}_{G_0^{\lambda}} \text{Ad}_{G_\lambda^i} + \text{Ad}_{G_0^i} \text{ad}_{\mathbf{s}_i} \dot{\mathbf{q}}_i$ 
19    $\mathbf{J}_{[:,i]}^s = \text{Ad}_{G_0^i} \mathbf{s}_i$ 
20 end
21  $\mathbf{r}_0^{TCP} \leftarrow \mathbf{G}_0^n \mathbf{G}_n^{TCP}$ 
22  $\mathbf{J} = [\mathbf{I} \quad -[\mathbf{r}_0^{TCP}]] \mathbf{J}^s$ 
23  $\dot{\mathbf{r}}_0^{TCP} = \mathbf{J} \dot{\mathbf{q}}$ 
24  $\dot{\mathbf{J}} = [\mathbf{0} \quad -[\dot{\mathbf{r}}_0^{TCP}]] \mathbf{J}^s + [\mathbf{I} \quad -[\mathbf{r}_0^{TCP}]] \dot{\mathbf{J}}^s$ 
25 end

```

IV. CONCLUSIONS

This study has presented a sensitivity analysis of a PMSM-powered EMLA-driven HDMM, focusing on how varying payload masses impact performance metrics such as power, force, energy expenditure, and efficiency. The findings offer crucial insights into the behavior of these actuators under different loading conditions, providing an insight for the development of next-generation, fully-electrified HDMMs.

The key contributions of this research are:

- Introducing a mathematical model of a gear-equipped PMSM-powered EMLA. This model encompasses equivalent circuit representations for the inverter, EM, gearbox, screw mechanism, and load. By employing the analogy of force-to-voltage and speed-to-current, this framework facilitates a thorough understanding of the governing

dynamics and enables precise performance analysis of the EMLA.

- Assisting in the informed selection of EMLAs for each joint of the manipulator by analyzing the sensitivity of required force and delivered power with respect to the TCP payloads.
- Facilitating the optimal sizing of batteries required to ensure effective operation of electric HDMM, thereby enhancing their performance and efficiency.

These contributions are vital for appropriate selection of actuators and battery capacity, and paves the way for the design of high-performance, autonomous HDMMs capable of efficient and sustainable operation. Future research could expand this sensitivity analysis to encompass a broader range of manipulator designs and operational conditions.

REFERENCES

- [1] Paris Agreement. Paris agreement. In *report of the conference of the parties to the United Nations framework convention on climate change (21st session, 2015: Paris)*. Retrived December, volume 4, page 2017. HeinOnline, 2015.
- [2] Daniele Beltrami, Paolo Iora, Laura Tribioli, and Stefano Uberti. Electrification of compact off-highway vehicles—overview of the current state of the art and trends. *Energies*, 14(17):5565, 2021.
- [3] Fuad Un-Noor, Guoyuan Wu, Harikishan Perugu, Sonya Collier, Seungju Yoon, Mathew Barth, and Kanok Boriboonsomsin. Off-road construction and agricultural equipment electrification: Review, challenges, and opportunities. *Vehicles*, 4(3):780–807, 2022.
- [4] Joseph T Jose, Jayanta Das, Santosh Kr Mishra, and Gyan Wrata. Early detection and classification of internal leakage in boom actuator of mobile hydraulic machines using svm. *Engineering Applications of Artificial Intelligence*, 106:104492, 2021.
- [5] Mohammad Bahari, Alvaro Paz, Andrew S. Habib, and Jouni Mattila. Performance evaluation of an electromechanical linear actuator with optimal trajectories. In *2023 IEEE 97th Vehicular Technology Conference (VTC2023-Spring)*, pages 1–7, 2023.
- [6] Josef Markus Ratzinger, Simon Buchberger, and Helmut Eichlseder. Electrified powertrains for wheel-driven non-road mobile machinery. *Automotive and Engine Technology*, 6:1–13, 2021.
- [7] Farid Tootoonchian and Zahra Nasiri-Gheidari. Cogging force mitigation techniques in a modular linear permanent magnet motor. *IET Electric Power Applications*, 10(7):667–674, 2016.
- [8] Mehdi Heydari Shahna, Mohammad Bahari, and Jouni Mattila. Robust decomposed system control for an electro-mechanical linear actuator mechanism under input constraints. *International Journal of Robust and Nonlinear Control*, 2024.
- [9] Ramu Krishnan. *Permanent magnet synchronous and brushless DC motor drives*. CRC press, 2017.
- [10] Carlos Candelo-Zuluaga, Antonio Garcia Espinosa, Jordi-Roger Riba, and Pere Tubert Blanch. Pmsm design for achieving a target torque-speed-efficiency map. *IEEE Transactions on Vehicular Technology*, 69(12):14448–14457, 2020.
- [11] Kevin M Lynch and Frank C Park. *Modern robotics*. Cambridge University Press, 2017.
- [12] J.-M. Selig. *Geometric Fundamentals of Robotics*. Springer, New York, 2005.
- [13] Alvaro Paz and Gustavo Arechavala. Analytical differentiation of the articulated-body algorithm: a geometric multilinear approach. *Multibody System Dynamics*, 60(3):347–373, 2024.
- [14] R. Featherstone. *Rigid Body Dynamics Algorithms*. Springer-Verlag, New York, 2008.
- [15] Wen-Hong Zhu. *Virtual decomposition control: toward hyper degrees of freedom robots*, volume 60. Springer Science & Business Media, 2010.
- [16] Goran R Petrović and Jouni Mattila. Mathematical modelling and virtual decomposition control of heavy-duty parallel–serial hydraulic manipulators. *Mechanism and Machine Theory*, 170:104680, 2022.